Applied Geochemistry 33 (2013) 252–259

Contents lists available at SciVerse ScienceDirect

Applied Geochemistry

journal homepage: www.elsevier.com/locate/apgeochem

Sourcing sedimentary cherts with archaeological use through the combination of chromatographic and spectroscopic techniques

M. Olivares [a,*], M. Irazola [a], X. Murelaga [b], J.I. Baceta [b], A. Tarriño [c], K. Castro [a], N. Etxebarria [a]

[a] University of the Basque Country (UPV/EHU), Department of Analytical Chemistry, P.O. Box 644, E-48080 Bilbao, Basque Country, Spain
[b] University of the Basque Country (UPV/EHU), Department of Stratigraphy and Palaeontology, P.O. Box 644, E-48080 Bilbao, Basque Country, Spain
[c] National Research Centre on Human Evolution (CENIEH), E-09004 Burgos, Spain

ARTICLE INFO

Article history:
Received 24 June 2012
Accepted 19 February 2013
Available online 6 March 2013
Editorial handling by R. Fuge

ABSTRACT

The nature and distribution of organic matter in geological cherts of archaeological use can serve to estimate the sources and origins of some remains of lithic industry. For example, organic and biomarker analysis can provide information to allow a deeper insight into source catchment areas, artefact displacement or the way in which the artefacts were employed. In this work, soluble (bitumen) and insoluble (kerogen) organic matter were isolated from several chert samples with different depositional history and analysed by means of gas chromatography–mass spectrometry (GC–MS) and spectroscopic techniques such as infrared and Raman spectroscopy. Chemometric treatment of the results allowed observation of differences between organic matter content on the basis of the depositional setting of the cherts. Samples with a continental deposition seemed to preserve more organic matter with little alteration. The hydrocarbon profiles of these samples were dominated by high molecular weight *n*-alkanes, alkylcyclohexanes and isoprenoid groups which allowed distinguishing them from the rest of the analysed samples.

1. Introduction

One of the most typical issues that archaeologists have to deal with concerns the provenance of archaeological lithic items. Cherts are amongst the oldest sedimentary rocks on Earth and offer a remarkable record of well-preserved microfossils (Allwood et al., 2006a) which gives clues to understanding the origins of life on the planet or even allow archaeologists to investigate such diverse topics as mobility patterns, prehistoric migrations or possible commerce routes. One of the assumptions is based on the fact that the tools and artefacts were manufactured close to the site where they were found, which would mean short mobility routes and the exploitation of local resources. Another scenario would be that in which bulk chert nodules were transported from the source to the site of manufacture (Fernandes et al., 2008).

In a previous study of the same lithic materials as those discussed herein, the chemical and mineralogical features of the inorganic remains were investigated to determine the extent to which those characteristics were relevant for classifying different raw materials (Olivares et al., 2009). It was concluded that additional chemical information was required since the inorganic patterns found in different chert samples showed very subtle differences for classifying these samples.

It is well known that organic matter (OM) can provide information concerning depositional conditions (marine, terrestrial or lacustrine environments) and whether the environment was oxic or anoxic, etc. (Peters and Moldowan, 1993; Vandenbroucke and Largeau, 2007).

In the specific case of cherts, the marked grey or even black colour is associated with OM trapped during formation and the burial history of the host rock, though the presence of OM in such samples is still under discussion (Derenne et al., 2008). Broadly speaking, under favourable physical conditions, the OM is converted mainly into two broad fractions: extractable bitumen and insoluble kerogen (Killops and Killops, 2005). The bitumen fraction corresponds to the OM extracted using common organic solvents and contains *n*-alkanes, methylalkanes and complex polycyclic biomarkers such as hopanes and steranes. Kerogen is the insoluble fraction remaining after an organic solvent extraction and is comprised of various macerals.

Organic biomarker geochemistry potentially provides a powerful tool for investigating the environmental information concealed in geological samples (Peters and Moldowan, 1993). Abelson (P.H.) was among the first to suggest that the analysis of 'fossil bio-chemicals' might give clues to the evolution of early life (quoted by Brocks et al. (2003)). Numerous later studies have shown that identification of the OM trapped in cherts may also help identify their source areas, so that a link between the compositional traits of OM and the geochemical characteristics of the depositional settings in which the cherts were formed can be established based on the recognition of aliphatic hydrocarbons and especially on molecular biomarkers (Parnell et al., 2007; Šajnović et al., 2008). Biomarkers are molecular fossils that can be found in rocks and sediments and

* Corresponding author. Tel.: +34 94 601 5504; fax: +34 94 601 3500.
E-mail address: maitane.olivares@ehu.es (M. Olivares).

0883-2927/$ - see front matter © 2013 Elsevier Ltd. All rights reserved.
http://dx.doi.org/10.1016/j.apgeochem.2013.02.020

show little or no change in structure from their parent organic molecules preserving all depositional information. Although *n*-alkanes are not considered as biomarkers, their distribution patterns and specific parameters (e.g., Carbon Preference Index, CPI) allow discrimination among different chert samples based on the source of the OM input (Peters and Moldowan, 1993). Regarding biomarkers, hopanes and steranes are among the most ubiquitous biomarkers and can provide information about the studied material. In fact, steranes are indicative of the type of organic matter input whereas hopanes distribution may also be related to the depositional environment (Peters and Moldowan, 1993).

Biomarker analysis, however, is not an easy analytical task as they are present in sub-ppb quantities and their isolation requires efficient extraction procedures (Marshall et al., 2007). Chromatographic techniques, such as gas chromatography with flame ionisation detection (GC–FID), gas chromatography mass spectrometry (GC–MS) or multidimensional gas chromatography (GC × GC) are among the main techniques for bitumen analysis (Marshall et al., 2005; Allwood et al., 2006b; Herod et al., 2007). For kerogen analysis otherwise vibrational spectroscopic techniques (such as infrared or Raman spectroscopy), mass spectrometry (MS) analyses (such as pyrolysis–gas chromatography/mass spectrometry or thermogravimetric analysis/mass spectrometry) or direct elemental analysis have been used widely.

In the framework of a general study of geological and archaeological chert samples collected from different sources in northern Spain and southern France, the chemical characterisation of the cherts has been determined (Tarriño, 2006; Olivares et al., 2009). All these chert localities are recognised as being the sources or quarries of raw material for the manufacture of chert tools found in many archaeological sites across the north of Spain and southern France (Tarriño, 2006). However, the organic fraction in many of the samples was ignored. Therefore, in order to evaluate the potential value of the organic fraction to provide further information about the geological cherts with archaeological use, the main aims of this work were to determine the nature of the OM in chert samples from different rock formations of different ages via determination of the distribution patterns of organic components, which would thereby allow the investigation of any type of correlation with the depositional setting (i.e., the source of chert).

2. Experimental

2.1. Samples

The samples were collected from different formations of Cretaceous to Cenozoic age outcropping across the Vasco-Cantabrian and Ebro Basins in the western Pyrenees. The chert-bearing units are of sedimentary origin and were deposited in different continental, shallow marine and deep marine lithologies. Most of the formations are characterised by a dominance of carbonate lithologies in the form of different types of fossiliferous to fine-grained limestones, marly limestones and marlstones. Chert samples from Loza and Tobera (Araba, Basque Country), Cucho (Trebiño County, Burgos) and Ablitas (Navarre) are all of continental origin, as they occur within successions of well-stratified lacustrine limestones and marlstones. They vary in age between early Eocene (Loza and Tobera) and early to middle Miocene (Cucho and Ablitas). Differences in the same geological deposition are reflected in cherts collected from Cucho, whereby three types of cherts: nodular chert, silcrete or massive brechoid chert or laminar chert occur (Tarriño, 2006). The Kurtzia cherts are hosted within Cenomanian to Maastrichtian deep marine limestone-marl alternations exposed along sea cliffs near the village of Barrika (Biscay, Basque Country). Finally, other chert samples from Mouguerre and Bearne (SW France) that are equivalent in age and environmental sedimentary formation to the Late Cretaceous Barrika chert were also sampled.

The cherts are of early diagenetic origin and usually occur as cm to dm-thick irregular to roundish nodules within the host limestones. In addition, cherts of continental origin from the Cucho, Arrieta, Ablitas and Loza sites may also occur as laterally discontinuous levels along bedding planes, which eventually reach up to 1 m in thickness.

2.2. OM isolation

The samples were first cleaned with organic solvent (CH_2Cl_2) to minimise cross contamination and were ground to a fine homogeneous representative powder. The bitumen fraction was isolated by means of an optimised method (Olivares et al., 2010) and the kerogen fraction was isolated by way of a standardised procedure (Durand and Nicaise, 1980).

In brief, a representative aliquot of each sample (ca. 2 g) was treated with 15 mL of extractant solvent mixture consisting of CH_2Cl_2/hexane/acetone (15 mL; 6/3/1; all HPLC grade, 99.8%) using a microwave digestion system (CEM Mars 6, at 110 °C maintained for 20 min). The extract was centrifuged at 2000 rpm for 15 min and the supernatant was evaporated to dryness under a N_2 flow and re-dissolved in 200 μL of hexane (HPLC grade, LabScan, Dublin, Ireland). Deuterated docosane (D_{46}) and dotriacontane (D_{66}) were added (1 μg/g each) as internal standards.

The kerogen was isolated from the solid residue following the standard procedure of Durand and Nicaise (1980). HCl 6 M (purity of 37%; Tracepur, Merck) was added to dissolve carbonate and, a mixture of HF (purity 49%, Merck) and HCl 6 M (1:1) was then added to the residue to eliminate clay minerals, quartz and silicates. Afterwards the formation of neofluorides was avoided by rinsing several times with hot distilled water. Lastly, a new HCl 6 M addition eliminated the excess of HF to avoid the formation of non-soluble F^- ions. The black residue obtained was filtered to dryness and dried at 100 °C under a N_2 flow.

2.3. Analysis of bitumen fraction

The bitumen fraction was analysed by means of GC–MS using a 6890N Agilent gas chromatograph coupled to a 5973N Agilent mass spectrometer with a 7683 Agilent autosampler. Two microlitres of the sample were injected in splitless mode at 300 °C into a HP-5ms (30 m × 0.25 mm, 0.25 μm, Agilent) column. The temperature programme was as follows: 60 °C (0.5 min), 120 °C at 20 °C min^{-1} and then to 300 °C at 6 °C min^{-1} (held 15 min). Helium (99.9995%; Carburos Metálicos, Barcelona, Spain) was used as a carrier gas at a constant pressure of 13.4 psi. The transfer line temperature was maintained at 310 °C, and the ion source and quadrupole at 230 °C and 150 °C, respectively. All the analyses were performed in SCAN mode. The *n*-alkane distribution was determined in single ion monitoring (SIM) mode using the most abundant *m*/*z* fragments (*m*/*z* 57, 71, 85). Biomarkers were identified from the mass spectra and comparison of retention times with those of standard compounds and literature data (Fleck et al., 2002; Šajnović et al., 2008). Sterane and terpane distributions were identified using their characteristic *m*/*z* 217 and *m*/*z* 191 fragmentograms respectively (Peters and Moldowan, 1993).

In order to take advantage of the multivariate analysis of the gas-chromatographic elution profiles, the retention time locking (RTL) feature was implemented in the separation programme (Bartolomé et al., 2007; Etxebarria et al., 2009). The RTL option was calibrated using a standard solution of a mixture of *n*-alkanes (C_{16}–C_{44}) by following the instructions of the GC instrument manufacturer. These are based on five runs carried out at different pressures (−20% and 20% of the standard pressure). The ChemStation

software (Agilent) automatically fits the retention time (t_R) of the selected standard compounds vs. pressure and, according to that, the retention time of the *n*-alkane present in the middle of the chromatogram is locked. In this case, the working pressure for this GC method at the top of the column was ca. 13.4 psi and the t_R of the standard was 20.94 min. Once the above *n*-alkane was locked, the retention times of all the resolved peaks were highly repetitive, allowing multivariate analysis of the chromatograms without realignment of the chromatograms.

2.4. Analysis of kerogen fraction

The kerogen fraction was characterised by means of Raman and infrared (IR) spectroscopy. The IR equipment was a Jasco-6300 spectrometer (Jasco, Japan) used in reflectance mode with an attenuated total reflectance (ATR) module (Pike Technologies, Madison, WI, USA). ATR-IR spectra were taken directly without any pre-treatment of the sample between 600 and 4000 cm^{-1} with a resolution of 4 cm^{-1}, a collection time of 4 s and 40 accumulations. The spectra were converted from reflectance to transmittance mode using the Jasco software in order to meet correct assignment of infrared bands.

A Renishaw InVia Raman spectrometer coupled to a Leica DMLM microscope was used for Raman spectroscopy analyses, and has a spatial resolution of 2 μm for the 50× objective. A 514 nm laser was used and the laser power was reduced to avoid photo decomposition of the sample (burning). Acquisition time was of 10 s and 10 scans were accumulated at the 10% of the maximum laser power in the spectral window from 200 cm^{-1} to 2200 cm^{-1}.

2.5. Data analysis

The whole chromatograms obtained for the bitumen fractions were compared using principal component analysis (PCA). The target *m*/*z* values (i.e., *m*/*z*: 191 for hopanes) were extracted from the scan mode chromatograms in the region in which the hopanes elute (i.e., 32–48 min). Following the procedure used by Bartolomé et al. (2007), all the information was loaded into The Unscrambler programme (v.7.6, Camo, Norway) in a table format with 14 chromatograms and 1710 retention times, where each row was the *m*/*z* 191 chromatogram for each sample and the columns the retention times. Before multivariate analysis of the data, it was necessary to normalise the chromatograms to eliminate any variation due to the total bitumen concentration and to focus on the information regarding the relative hopane distribution. Among the different options, mean normalisation was used, which consists of dividing each row of data matrix by its average value. The PCA models were built with centred data and using full cross-validation.

The Raman spectra of kerogen fractions were pre-processed using the Grams 32 (Galactica, Thermo, US) software package. The deconvolution was done by splitting the spectrum into an addition of Gaussian and Lorentzian functions by using Curvefit routine implemented in Grams32 software. The best model was achieved when statistic Chi-squared was optimised, taking into account the r^2 correlation as well as obtaining a coherent model, that is, with the absence of negative or redundant peaks.

3. Results and discussion

3.1. Bitumen analysis

3.1.1. n-Alkanes

n-Alkanes are ubiquitous in geological samples and they have been identified (*m*/*z*: 57, 71, 85) in all analysed chert samples. Based on the analytical results of *n*-alkanes the following parameters were obtained.

(i) The ratio between light and heavy *n*-alkanes calculated as follows can be indicative of the type of OM input (Peters and Moldowan, 1993):

$$\frac{\sum 1}{\sum 2} = \frac{\sum(C_{16}H_{34} - C_{22}H_{46})}{\sum(C_{23}H_{48} - C_{35}H_{72})} \quad (1)$$

A marked dominance of light *n*-alkanes ($C_{16}H_{33}$–$C_{22}H_{45}$), i.e., a high value of the $\sum 1/\sum 2$ ratio, can be attributed to a suboxic deposition of algal biomass or to a bacterial input during the depletion of silica and can be related to a marine or saline environment. On the other hand, distributions characterised by an increase in the relative proportion of higher *n*-alkanes ($C_{23}H_{48}$–$C_{35}H_{70}$), i.e., a lower value of $\sum 1/\sum 2$, are related to an origin from terrestrial higher plants.

(ii) The odd/even preference is another parameter which can be used as a source indicator. The CPI, a numerical expression of the odd/even *n*-alkanes distribution, provides information about the OM maturity (Peters and Moldowan, 1993):

$$\mathrm{CPI} = 1/2\left\{\frac{(n-C_{25}+n-C_{27}+n-C_{29}+n-C_{31}+n-C_{33})}{(n-C_{24}+n-C_{26}+n-C_{28}+n-C_{30}+n-C_{32})} + \frac{(n-C_{25}+n-C_{27}+n-C_{29}+n-C_{31}+n-C_{33})}{(n-C_{26}+n-C_{28}+n-C_{30}+n-C_{32}+n-C_{34})}\right\}$$

Values significantly above 1.0 (odd preference) indicate low thermal maturity. Values of 1.0 suggest, but do not prove, that the bitumen fraction is mature and finally values below 1.0 (even preference) are unusual and typify low maturity samples from carbonate or hypersaline environments.

Table 1 and Fig. 1 summarise the *n*-alkane results (concentration of *n*-alkanes in ng/g and the values of those geochemical parameters, i.e., $\sum 1/\sum 2$ and CPI, for each analysed chert sample) in which different *n*-alkane distribution patterns can be observed. A subset of samples collected from Cucho, massive brechoid or silcrete cherts, are characterised by low $\sum 1/\sum 2$ (<0.2) and high CPI values (>3.0) (see Fig. 1, this data set is circled on the figure with a dotted line). These values suggest a low maturity (CPI > 1.0) and terrestrial plants are the most likely source of the OM (odd preference). The rest of the samples (see Fig. 1, samples circled by a solid line), including Cucho laminar and nodular cherts, are aligned in a wide range of $\sum 1/\sum 2$ values (from 0.1 to 0.7 in Cucho but up to 2.5 in Barrika) but at constant CPI value (slightly above 1.0). This would suggest a thermal maturity of the OM but a wide range of algae or bacteria inputs and salinities. In this sense, cherts collected from Barrika, all show a higher preference for light *n*-alkanes, suggesting a predominance of algal biomass and a net marine environment and those collected in Loza would suggest the inputs of terrestrial plants.

3.1.2. Hopanes

Steranes and hopanes were only detected in chert samples collected in Cucho and Loza cherts, being close to the detection limit (signal-to-noise ratio < 10) for the rest of the samples, so those samples were not included in the comparison.

Since the hopanes (diagnostic ions *m*/*z*: 177, 191, 205) were present in high abundance in all the Cucho cherts, the pre-processed chromatograms were compared using PCA (see Section 2.5 for details). In this way, the first two PCs explained up to 90% of the total variance in which two different sample groups could be easily differentiated (see Fig. 2). As can be seen in Fig. 3, where two chromatograms from different chert samples are plotted, the different

Table 1
Geochemical data of *n*-alkanes derived from the analysed chert samples.

Depositional setting	Geological setting	Sample	C_{tot}(ng/g) (2s)	$\sum 1/\sum 2$	CPI
Deep marine	Barrika	BRK 2	455 ± 109	2.46	0.81
		BRK 3	213 ± 51	2.28	1.33
		BRK 4	252 ± 60	1.15	1.55
	Mouguerre	MOU 2	314 ± 94	0.41	0.94
		MOU 5	364 ± 105	0.24	0.93
		MOU 6	301 ± 90	0.27	1.08
		MOU 7	317 ± 91	0.22	1.02
	Bearn	BEARN 1	2092 ± 418	0.19	1.19
		BEARN 2	1366 ± 273	0.19	0.77
Lacustrine	Tobera	TOB 1	215 ± 61	0.48	1.52
		TOB 2	278 ± 80	0.34	1.09
		TOB 3	297 ± 83	0.35	1.19
		TOB 4	209 ± 61	0.26	1.06
		TOB 5	337 ± 97	0.29	1.23
	Loza	LOZ 1	1997 ± 260	0.12	1.09
		LOZ 2	875 ± 114	0.28	1.2
		LOZ 3	714 ± 93	0.41	1.06
	Cucho massive-brechoid	CU 1	3045 ± 680	0.09	3.59
		CU 2	1511 ± 331	0.13	3.41
		CU 3	3446 ± 762	0.09	3.06
		CU 9	887 ± 199	0.17	4.53
		CU 10	642 ± 134	0.16	4.89
		CU 4	6566 ± 1152	0.63	1.28
	Cucho laminar	CU 5	3310 ± 596	0.64	1.17
		CU 6	2812 ± 510	0.65	1.18
		CU 11	664 ± 199	0.5	1.24
	Cucho nodular	CU 13	646 ± 192	0.62	1.37
		CU 15	637 ± 191	0.59	1.29
		CU 16	584 ± 175	0.52	1.33
	Ablitas	ABL 3	551 ± 131	0.26	1.05

patterns observed between the laminar and the rest of cherts were attributed to a different hopane distribution. The identification of hopanes responsible for the variance in this distribution was carried out using mass spectra. The assignment of the peaks is detailed in Table 2 and was based on literature data and interpretation of mass spectra (Peters and Moldowan, 1993; Fleck et al., 2002; Šajnović et al., 2008).

The laminar cherts were characterised by 17α(H),21β(H) hopane, the presence of gammacerane and a C_{35}/C_{34} homohopane ratio > 1 (Fig. 3b). Gammacerane is a major biomarker in many bitumens of lacustrine origin and high abundances indicate relatively saline/hypersaline and anoxic/suboxic conditions during deposition. Hypersaline conditions in lacustrine environments are usually the result of enhanced stratification of the bottom water or periodic episodes of intense evaporation during the evolution of the lake. A remarkable high abundance of gammacerane was observed in the laminar cherts, which are located in the upper (terminal) part of the lacustrine limestone succession. In contrast, the abundance in the nodular and massive-brechoid cherts, located at deeper lithological intervals, was much lower.

In addition, the presence of gammacerane, laminar cherts were characterised by a high C_{35} homohopane index or predominance of higher homohopane homologues, which may be related to extensive bacterial activity in the depositional environment. This feature is in concordance with the geological evidence, as fossil laminar algae and overgrowths are abundant in the upper part of the Cucho lacustrine unit.

The hopane distribution for massive-brechoid and nodular cherts is dominated by 17α(H),21β(H) norhopane and 17α(H),21β(H) hopane but, in this case, the relative abundance of the extended homohopanes > C_{31} decreases progressively (Fig. 3a). This distribution is associated with oxic environments and their relative low abundance compared to 17α(H),21β(H) hopane is characteristic of non-marine deposits.

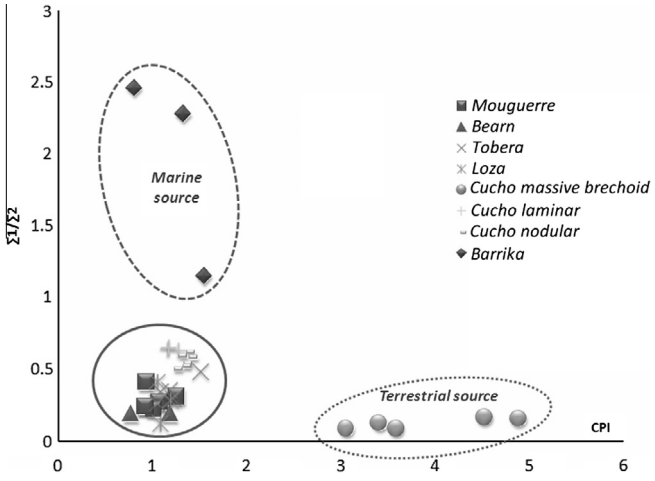

Fig. 1. Light/heavy *n*-alkane ratios ($\sum 1/\sum 2$) vs. Carbon Preference Index (CPI) diagram showing the different *n*-alkane profiles found in the analysed chert samples.

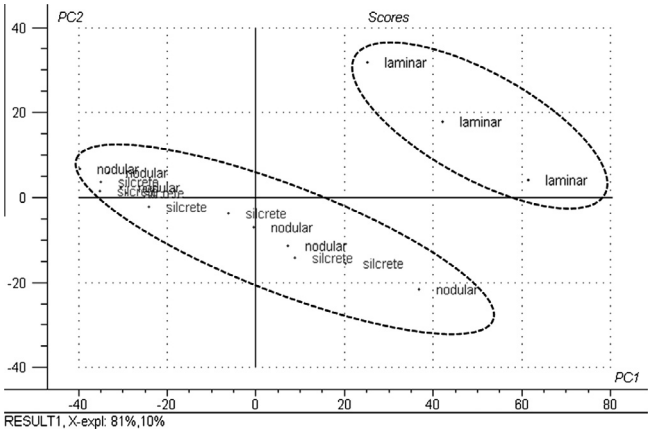

Fig. 2. Scores plot (PC1 vs. PC2) of *m*/*z* 191 chromatographic fragmentograms analysed by principal components analysis for Cucho samples (laminar, silcrete or massive-brechoid and nodular).

3.1.3. Steranes

The analysis of steranes (diagnostic ions *m*/*z*: 217 and the molecular ions *m*/*z*: 372, 386, 400 C_{27}, C_{28} and C_{29} sterane isomers, respectively) can provide information about the OM type, for example, the ratios $C_{27}/C_{29} > 1$, $C_{27}/C_{29} < 1$ and $C_{28}/C_{29} > 1$ between regular steranes have been used as indicators of marine, terrigenous and diatomaceous OM input, respectively. The relative contents (%) of C_{27}, C_{28} and C_{29} regular steranes were calculated from the peak areas of C_{27}, C_{28} and C_{29}.

The samples were typically very low in steranes with the low sterane/hopane ratios values suggesting terrigenous OM. Nevertheless, using sterane ternary diagrams (constructed from C_{27}, C_{28} and C_{29} sterane ratios) differences in OM input can be found (Fig. 4).

Traditionally lacustrine environments are thought to show a higher concentration of C_{28} steranes (Peters and Moldowan, 1993). However, the low relative abundance in the regular C_{28} steranes in the chert samples suggests the absence of true deep lacustrine phytoplankton, probably because of very shallow water conditions. The laminar samples were characterised by higher

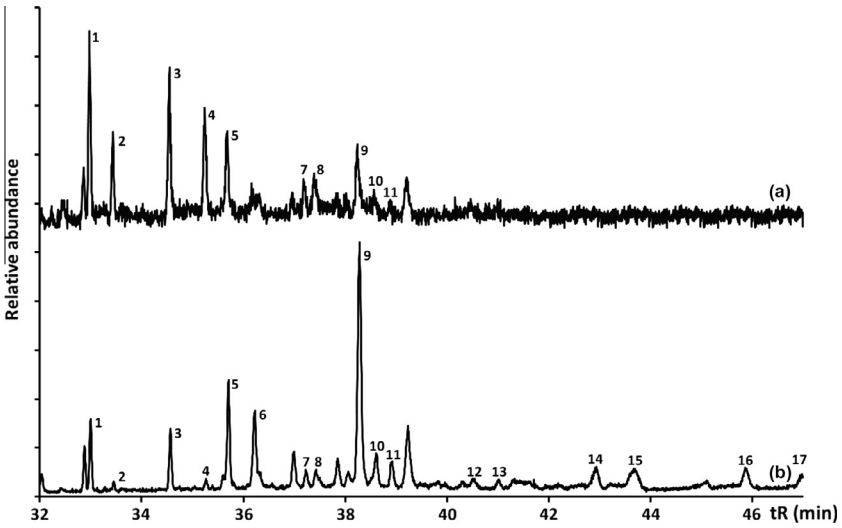

Fig. 3. Typical hopanoid distributions corresponding to the analysed chert samples in *Cucho* and determined $m/z = 191$. Refer to Table 2 for peak assignments. (a) Massive brechoid and (b) laminar.

Table 2
Peak assignment for hopanes (m/z: 191) in Fig. 3.

Peak	Hopane name	Carbon number	Ion molecular m/z
1	18α(H)-22,29,30-Trisnorhopane (Ts)	C_{27}	370
2	17α(H)-22,29,30-Trisnorhopane (Tm)	C_{27}	370
3	17α(H),21β(H)-norhopane	C_{29}	398
4	17β(H),21α(H)-normoretane	C_{29}	398
5	17α(H),21β(H)-hopane	C_{30}	412
6	17β(H),21α(H)-moretane	C_{30}	412
7	22S-17α(H),21β(H)-homohopane	C_{31}	426
8	22R-17α(H),21β(H)-homohopane	C_{31}	426
9	Gammacerane	C_{30}	412
10	22S-17α(H),21β(H)-bishomohopane	C_{32}	440
11	22R-17α(H),21β(H)-bishomohopane	C_{32}	440
12	22S-17α(H),21β(H)-trishomohopane	C_{33}	454
13	22R-17α(H),21β(H)-trishomohopane	C_{33}	454
14	22S-17α(H),21β(H)-tetrakishomohopane	C_{34}	468
15	22R-17α(H),21β(H)-tetrakishomohopane	C_{34}	468
16	22S-17α(H),21β(H)-pentakishomohopane	C_{35}	482
17	22R-17α(H),21β(H)-pentakishomohopane	C_{35}	482

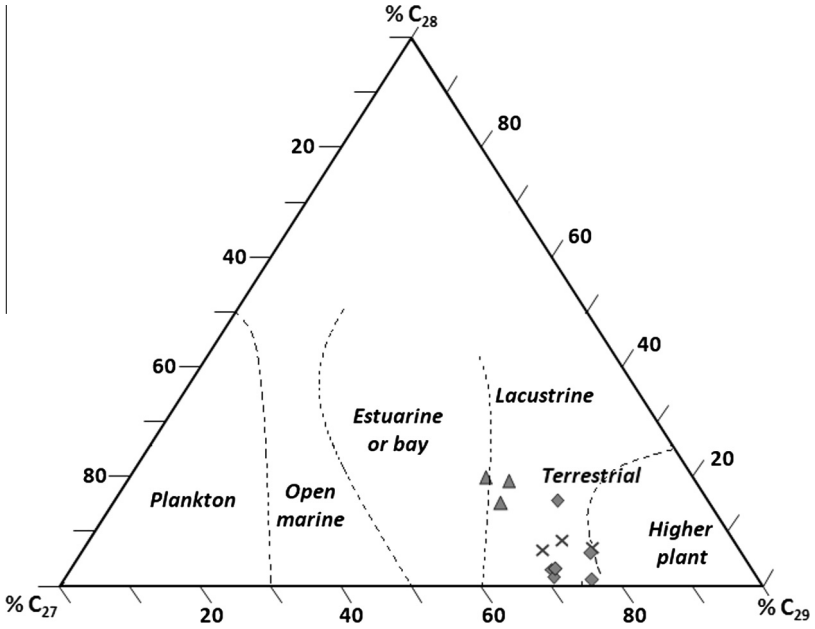

Fig. 4. Sterane ternary diagram as a function of sterol compositions in analysed chert samples collected in Cucho: laminar (▲), massive-brechoid (×) and nodular (♦). The dotted zone underlines the different environments characterised by sedimentology.

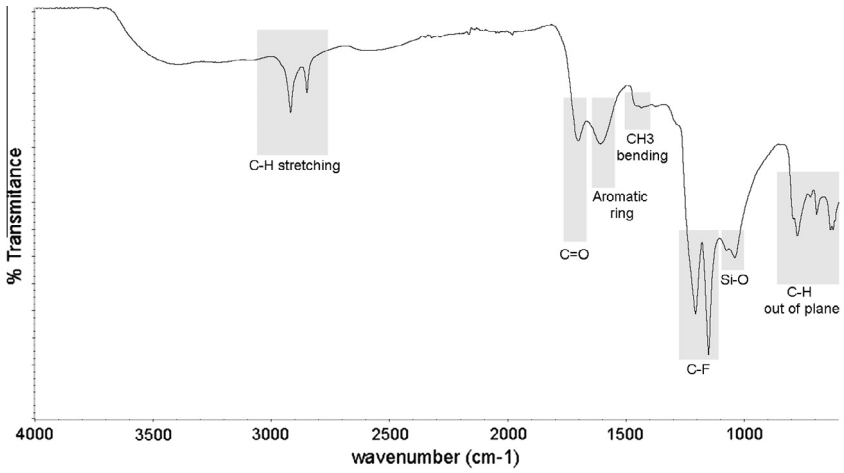

Fig. 5. ATR-IR spectra of isolated kerogen which shows the typical characteristic infrared bands of this compound.

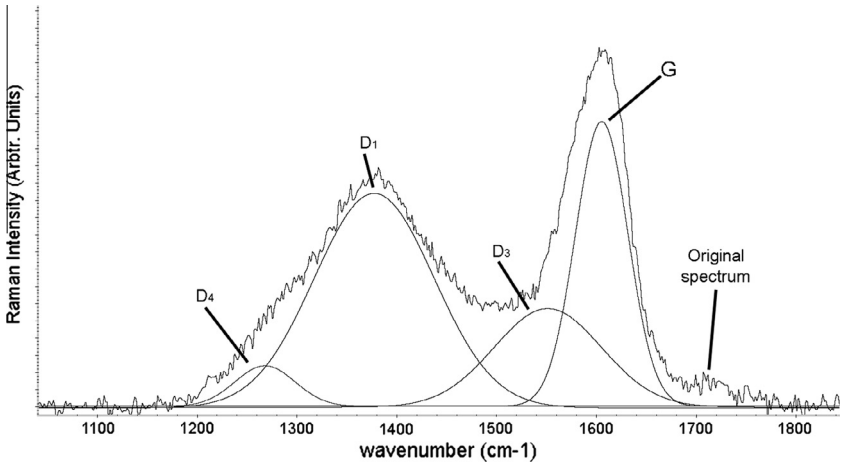

Fig. 6. Raman spectra of kerogen extract isolated from chert sample in which carbon Raman absorption bands can be identified.

amounts of C_{27} steranes, indicating a predominantly algal origin. On the other hand, massive-brechoid cherts were characterised by a higher abundance of C_{29} steranes. Such a distribution is related to a vascular plant source, which is in agreement with the previous conclusions from the *n*-alkane profiles of the massive-brechoid cherts. Finally, regardless of the lower content of OM in the nodular cherts, they exhibit a distribution of both hopanes and steranes similar or very similar to the massive-brechoid cherts. From these hopane and sterane fingerprints, it can be proposed that the low terrestrial OM input came from silica fluxes that allowed the migration of terrestrial OM from adjacent strata.

3.2. Kerogen analysis

Among other spectroscopic techniques, IR spectroscopy has been widely used to provide insight into the composition and structure of kerogen (Lis et al., 2005). The kerogen fraction was directly characterised by means of ATR-IR and the infrared bands were identified by comparison with published spectra (Durand and Nicaise, 1980).

The ATR-IR spectrum of a Cucho chert is shown in Fig. 5 and contains the following IR bands: aliphatic C—H stretching region (3000–2800 cm^{-1}), carbonyl/carboxyl band (~1700 cm^{-1}), aromatic ring stretching (~1600 cm^{-1}), CH_2 and CH_3 bending modes (~1450 cm^{-1}) and aromatic C—H out-of-plane deformation bands (700–900 cm^{-1}). There is another band (~1000 cm^{-1}) corresponding to Si—O vibrational modes resulting from residual silica. Furthermore, bands from neofluorides (~1100–1200 cm^{-1}) formed during the kerogen isolation are present, but these bands do not overlap with any other key bands.

ATR spectra of the extracted fraction of chert samples from other sites are not displayed since they are essentially featureless, as the only absorption band in the collected spectra is the Si—O vibrational mode due to the residues of non-dissolved SiO_2. This would be in agreement with the information obtained from bitumen analysis isolated from Cucho. Besides IR spectroscopy, Raman spectroscopy can be used to study carbonaceous geological materials (Jehlička et al., 2003). In this case also, only the samples characterised by means of ATR-IR spectroscopy were measured using micro-Raman spectroscopy. As an example, the Raman spectra of the kerogen fraction isolated from a Cucho chert is illustrated in Fig. 6. Several measurements were carried out to check the homogeneity of the kerogen fraction and comparable spectra were obtained. The stacked Raman spectra show pronounced bands at 1350 cm^{-1} (D band) and 1600 cm^{-1} (G band) corresponding to C (Allwood et al., 2006b; Jehlička et al., 2003; Marshall et al., 2007).

When spectrum deconvolution was carried out (see Section 2.5 for data analysis details), it was possible to distinguish all different D bands, as shown in Fig. 6. According to Allwood et al. (2006b), for an ideal graphite crystal only one first order band, the G (graphite) band, is exhibited at 1580 cm^{-1}. However, disordered carbona-

ceous material shows the D or defect bands characteristic of disordered sp^2 carbons. It is known that the relative intensity of D bands in relation to the G band decreases with increasing order in the graphitic structure (i.e., through metamorphism). Those D bands can be denoted as follows:

i. *D1 (1350 cm^{-1})*: The most intense D band. It is suggested to arise from graphene layer C atoms in the immediate vicinity of a lattice disturbance such as the edge of a graphene layer or a heteroatom.
ii. *D2 (1620 cm^{-1})*: Observed as a shoulder on the G band. Assigned to a lattice vibration involving graphene layers at the surface of a graphite crystal.
iii. *D3 (1550 cm^{-1})*: Assigned to the amorphous C fraction of organic molecules, fragments or functional groups.
iv. *D4 (1200 cm^{-1})*: Observed as a shoulder on the D1 band. Tentatively attributed to sp^2–sp^3 bonds or C—C and C=C stretching vibrations of polyene like structures.

In the spectrum in Fig. 6 it is possible to observe the D1 (1377 cm^{-1}), D3 (1551 cm^{-1}) and D4 (1267 cm^{-1}) bands together with the G band (1605 cm^{-1}). The maturity of the carbonaceous material can be examined on the basis of the width of the G band (full width at half maximum, W_G) and the relative intensity of the G and D bands (I_{D1}/I_G and $I_{D1}/(I_{D1} + I_G)$) of the deconvoluted spectra. In addition, those parameters have been shown to correlate with the amount of structural order in the carbonaceous matter (Cuesta et al., 1994).

Unfortunately, as with ATR-IR analysis, most of the Raman spectra collected from the extracted kerogen fractions were featureless and thus, only the kerogen fraction from a Cucho chert could be analysed by means of Raman spectroscopy. Therefore, it was not possible to compare the maturity of the samples. However, if the data observed for the Cucho sample ($W_G = 61.9$ and $I_{D1}/(I_{D1} + I_G) = 0.43$) are compared with those obtained by Marshall et al. (2007) and Allwood et al. (2006b), the obtained values might suggest that the kerogen corresponds to a highly disordered carbonaceous material, i.e., to a relatively low maturity, which agrees with the interpretation given from the analysis of the bitumen fraction of this type of chert.

4. Conclusions

The features derived from organic analysis are complementary to those obtained from inorganic analysis of the geological and archaeological cherts (Olivares et al., 2009). In this sense, the analysis of both extractable and insoluble OM provide valuable information about the environmental setting in which the cherts were formed as well as the type of OM that was trapped in the siliceous matrix.

In fact, the *n*-alkane distributions provide the first evidence of the type of source (i.e., depositional setting characteristics) in terms of, for example, marine or lacustrine cherts. In this sense, geological chert samples from Barrika can be differentiated from the cherts collected in Loza after the evaluation of the preference of light or heavy *n*-alkanes, i.e., a predominance of light *n*-alkanes for the first case suggesting a net marine depositional setting and a predominance of heavier *n*-alkanes for the second case suggesting the inputs of terrestrial plants and, therefore, a terrestrial environment.

In addition to this, biodegradation, maturation or migration of OM are reflected in the spectral fingerprints. For example, featureless mass spectra but particularly IR and Raman spectra, and a lack of odd or even predominance can be found in mature OM. Biomarker analysis can provide, in these situations, reliable information as shown in the obtained results. Both hopane and sterane distributions in the analysed chert samples have provided geochemical clues to distinguish between different types of chert samples with archaeological use. Thus, in the same depositional setting different chert samples were identified based on their type of organic matter biomass. The analysis of biomarker patterns has allowed classifying successfully chert samples collected in the Basque Cantabrian region. Thus, this methodology can be useful for the identification of the source of the raw geological material used to make archaeological chert pieces.

In order to extend this study to archaeological artefacts it needs to be considered that the process involves the destruction of the sample. This often means that the analysis has to be accomplished with chert splinters obtained in the quarries or valueless fragments. Thus, the characterisation of raw material of archaeological remains should be used in further research in order to deduce the depositional origin of the artefacts.

Acknowledgements

This work was supported by the Research Project CGL2008-00009/BTE of the Spanish Ministry of Science and Innovation and the funds dedicated to high-performance research groups (IT-245-07). The authors are grateful to the LASPEA unit of the General Research Services (SGIker) of the University of the Basque Country.

References

Allwood, A.C., Walter, M.R., Kamber, B.S., Marshall, C.P., Burch, I.W., 2006a. Stromatolite reef from the early Archaean era of Australia. Nature 441, 714–718.
Allwood, A.C., Walter, M.R., Marshall, C.P., 2006b. Raman spectroscopy reveals thermal palaeoenvironments of c. 3.5 billion-year-old organic matter. Vib. Spectrosc. 41, 190–197.
Bartolomé, L., Deusto, M., Etxebarria, N., Navarro, P., Usobiaga, A., Zuloaga, O., 2007. Chemical fingerprinting of petroleum biomarkers in biota samples using retention-time locking chromatography and multivariate analysis. J. Chromatogr. A 1157, 369–375.
Brocks, J.J., Buick, R., Logan, G.A., Summons, R.E., 2003. A reconstruction of Archean biological diversity based on molecular fossils from the 2.78–2.45 billion year old Mount Bruce supergroup, Hamersley basin, western Australia. Geochim. Cosmochim. Acta 67, 4289–4319.
Cuesta, A., Dhamelincourt, P., Laureyns, J., Martínez-Alonso, A., Tascon, J.M.D., 1994. Raman microprobe studies on carbon materials. Carbon 32, 1523–1532.
Derenne, S., Francois, R., Skrzypczak-Bondeuelle, A., Gourier, D., Binet, L., Rouzaud, J.N., 2008. Molecular evidence for life in the 3.5 billion year old Warrawoona chert. Earth Planet. Sci. Lett. 272, 476–480.
Durand, B., Nicaise, G., 1980. Kerogen Insoluble Organic Matter from Sedimentary Rocks. Technip, Paris.
Etxebarria, N., Zuloaga, O., Olivares, M., Bartolomé, L.J., Navarro, P., 2009. Retention-time locked methods in gas chromatography. J. Chromatogr. A 1216, 1624–1629.
Fernandes, P., Raynal, J.P., Moncel, M.H., 2008. Middle Palaeolithic raw material gathering territories and human mobility in the southern Massif central, France. First results from a petro-archaeological study on flint. J. Archaeol. Sci. 35, 2357–2370.
Fleck, S., Michels, R., Ferry, S., Malartre, F., Elion, P., Landais, P., 2002. Organic geochemistry in a sequence stratigraphic framework: the siliciclastic shelf environment of Cretaceous series, SE France. Org. Geochem. 33, 1533–1557.
Herod, A.A., Bartle, K.D., Kandiyoti, R., 2007. Characterization of heavy hydrocarbons by chromatographic and mass spectrometric methods: an overview. Energy Fuel 21, 2176–2203.
Jehlička, J., Orban, U., Pokorn, J., 2003. Raman spectroscopy of carbon and solid bitumens in sedimentary and metamorphic rocks. Spectrochim. Acta A 59, 2341–2352.
Killops, S., Killops, V., 2005. Introduction to Organic Geochemistry, second ed. Blackwell Publishing, Oxford.
Lis, G.P., Mastalerz, M., Schimmelmann, A., Lewan, M.D., Stankiewicz, A., 2005. FTIR absorption indices for thermal maturity in comparison with vitrinite reflectance R0 in type-II kerogens from Devonian black shales. Org. Geochem. 36, 1533–1552.
Marshall, C.P., Kamali Kannangara, G.S., Alvarez, R., Wilson, M.A., 2005. Characterisation of insoluble charcoal in Weipa bauxite. Carbon 43, 1279–1285.
Marshall, C.P., Love, G.D., Snape, C.E., Hill, A.C., Allwood, A.C., Walter, M.R., Van Kranendonk, M.J., Bowden, S.A., Sylva, S.P., Summons, R.E., 2007. Structural characterization of kerogen in 3.4 Ga Archaean cherts from the Pilbara craton, western Australia. Precambrian Res. 155, 1–23.

Olivares, M., Tarriño, A., Murelaga, X., Baceta, J.I., Castro, K., Etxebarria, N., 2009. Non-destructive methods to study the distribution of geological and archaeological chert samples. Spectrochim. Acta A 73, 492–497.

Olivares, M., Vallejo, A., Irazola, M., Murelaga, X., Baceta, J.I., Tarriño, A., Etxebarria, N., 2010. Optimisation of focused ultrasound extraction (FUSE) and microwave-assisted extraction (MAE) of hydrocarbons in geological chert samples. Talanta 83, 605–612.

Parnell, J., Bowden, S., Andrews, J.T., Taylor, C., 2007. Biomarker determination as a provenance tool for detrital carbonate events: fingerprinting quaternary glacial sources into Baffin bay. Earth Planet. Sci. Lett. 257, 71–82.

Peters, K.E., Moldowan, J.M., 1993. The Biomarker Guide. Interpreting Molecular Fossils in Petroleum and Ancient Sediments. Prentice Hall, New Jersey.

Šajnović, A., Stojanović, K., Jovančićević, B., Golovko, A., 2008. Geochemical investigation and characterisation of Neogene sediments from Valjevo-Mionica basin (Serbia). Environ. Geol. 254, 1260–1273.

Tarriño, A., 2006. El sílex en la Cuenca Vasco-Cantábrica y Pirineo Navarro: Caracterización y su aprovechamiento en la prehistoria. Secretaria General Técnica, Ministerio de Cultura, Spain.

Vandenbroucke, M., Largeau, C., 2007. Kerogen origin, evolution and structure. Org. Geochem. 38, 719–833.